Inorganic Chemistry

Article

pubs.acs.org/IC

NMR and Electron Paramagnetic Resonance Studies of $[Gd(CH_3CN)_9]^{3+}$ and $[Eu(CH_3CN)_9]^{2+}$: Solvation and Solvent Exchange Dynamics in Anhydrous Acetonitrile

Gabriella Bodizs[†] and Lothar Helm*

Ecole Polytechnique Fédérale de Lausanne (EPFL), Institut des sciences et ingénierie chimiques, EPFL-BCH, CH-1015 Lausanne, Switzerland

Supporting Information

ABSTRACT: Homoleptic acetonitrile complexes $[Gd(CH_3CN)_9][Al(OC(CF_3)_3)_4]_3$ and $[Eu(CH_3CN)_9][Al(OC(CF_3)_3)_4]_2$ have been studied in anhydrous acetonitrile by ^{14}N- and ^1H NMR relaxation as well as by X- and Q-band EPR. For each compound a combined analysis of all experimental data allowed to get microscopic information on the dynamics in solution. The second order rotational correlation times for $[Gd(CH_3CN)_9]^{3+}$ and $[Eu(CH_3CN)_9]^{2+}$ are 14.5 ± 1.8 ps and 11.8 ± 1.1 ps, respectively. Solvent exchange rate constants determined are $(55 \pm 15) \times 10^6\ s^{-1}$ for the trivalent Gd^{3+} and $(1530 \pm 200) \times 10^6\ s^{-1}$ for the divalent Eu^{2+}. Surprisingly, for both solvate complexes CH_3CN exchange is much slower for the less strongly N-binding acetonitrile than for the more strongly coordinated O-binding H_2O. It is concluded that this exceptional behavior is due to the extremely fast water exchange, whereas the exchange behavior of CH_3CN is more regular. Electron spin relaxation on the isoelectronic ions is much slower than on the O-binding water analogues. This allowed a precise determination of the hyperfine coupling constants for each of the two stable isotopes of Gd^{3+} and Eu^{2+} having a nuclear spin.

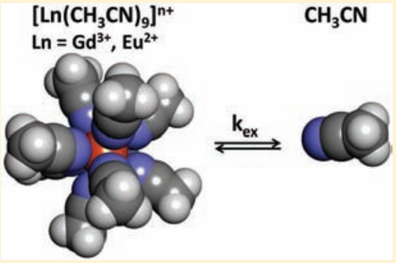

INTRODUCTION

Since Swift and Connick[1,2] described in 1962 for the first time equations for NMR line broadening in dilute solutions of paramagnetic ions, many studies on solvent exchange reactions in aqueous as well as nonaqueous solvents have been published in literature.[3] However, relatively few solvent exchange studies on homoleptic solvent complexes of lanthanide ions have been carried out so far. Two main reasons for this deficit of investigations are the short residence times of solvent molecules in the first coordination sphere of lanthanide ions[3] and the difficulty to obtain true homoleptic compounds in solution.[4] In contrast to that, many water exchange rate constants have been measured in the past two decades on lanthanide complexes with one inert chelating ligand and one or two first sphere water molecules.[3] This interest is largely caused by the use of these substances as magnetic resonance imaging (MRI) contrast agents or as luminescent biosensors.[5]

The 15 trivalent lanthanide ions, commonly denoted as Ln^{3+}, represent the most extended series of chemically similar metal ions. As a consequence of the progressive filling of the imperfectly shielded 4*f* orbitals, a smooth decrease of the ionic radius from La^{3+} to Lu^{3+} (lanthanide contraction) is observed.[6,7] The geometry of the first coordination sphere of Ln^{3+} solvate complexes is mainly determined by the electrostatic attraction of negatively charged atoms on polar molecules by the strongly charged cation and by steric repulsion between the coordinated solvent molecules. A solvent affinity sequence for $Tb(ClO_4)_3$ and $Tb(NO_3)_3$ has been established by Bünzli et al.[4,8] on the basis of luminescence data: DMSO > DMF ≈ H_2O > $(CH_3)_2CO$ > CH_3CN. This series has also been proved to be valid for the $Eu(CF_3SO_3)_2$ complex.[9]

The weak solvent coordination makes acetonitrile Ln^{3+}-complexes ideal precursors to synthesize a wide range of compounds under nonaqueous conditions. Following the Eigen–Wilkins mechanism, which has been established for reactions on octahedral complexes in water, the replacement of a solvent molecule from the first coordination sphere of an ion is often the rate determining step in any complex formation reaction.[10] From the solvents in the above-mentioned affinity sequence the exchange of the most strongly coordinated dimethylsulfoxide (DMSO) solvent has been studied only for Gd^{3+} so far.[11] Water[12−16] and dimethylformamide (DMF)[17,18] solvent exchange rate constants have been measured for the heavy elements in the second half of the lanthanide series. For the light elements Pr^{3+} and Nd^{3+} only lower limits for water exchange rate constants have been published so far.[19] For the second part of the lanthanide series (Gd^{3+} to Yb^{3+}) the water exchange rate constants on the eight coordinated aqua-ion $[Ln(H_2O)_8]^{3+}$ decrease systematically from ∼$8 \times 10^8\ s^{-1}$ to ∼$5 \times 10^7\ s^{-1}$.[20] The studied water exchange reactions are associatively activated meaning that the transition state has an increased coordination number of nine. The exchange rate constants for DMF, measured on Tb^{3+} to Yb^{3+}- ions first

Received: March 2, 2012
Published: May 3, 2012

decrease from Tb^{3+} to Ho^{3+} and then increase again up to Yb^{3+}.[17] This behavior has been explained by a change in mechanism from a concerted mechanism with dissociative activation (I_d) to a limiting dissociative mechanism (D). The exchange reaction of coordinated water is faster than that of DMF for all studied lanthanide ions except for the smallest ion Yb^{3+}. Investigations on divalent lanthanide ions are still scarce and mainly restricted to Eu^{2+}.[9,16,21] The water exchange on $[Eu(H_2O)_7]^{2+}$ has been found to be extremely fast—it is the fastest directly measured so far by ^{17}O NMR. Using X-ray absorption fine structure (XAFS), coordination numbers of seven (H_2O) and eight (CH_3CN) have been determined for lanthanide solvate complexes using $CF_3SO_3^-$ as anion.[9,22]

No solvent exchange on lanthanides has been studied so far for the weakest solvent in the affinity sequence, CH_3CN. This is explained by the difficulty to synthesize homoleptic acetonitrile lanthanide complexes, since even the normally weakly coordinating counterions like ClO_4^- and $CF_3SO_3^-$ compete with CH_3CN ligands for coordination sites.[4,23] In a recent publication it has been shown that homoleptic $[Ln(CH_3CN)_x]^{n+}$ complexes can be synthesized in the solid state and in solution using the huge monocharged anion $[Al(OC(CF_3)_3)_4]^-$.[24] It has been found that the coordination number decreases from 9 at the beginning and in the middle of the lanthanide series (Nd^{3+} to Dy^{3+}) to 8 at the end of the series (Tm^{3+}). For the divalent Eu^{2+} a coordination number of 9 has been deduced. Here we present a variable magnetic field and temperature ^{14}N-, ^1H NMR and electron paramagnetic resonance (EPR) study of the isoelectronic $S = 7/2$ ions Gd^{3+} and Eu^{2+} in neat acetonitrile solution. The favorable paramagnetic properties of these two ions consisting in high magnetic moments and slow electron spin relaxation allow us to determine for the first time CH_3CN exchange rate constants on homoleptic lanthanide complexes in acetonitrile solution.

EXPERIMENTAL SECTION

General Remarks. All preparations and physical measurement were carried out with rigorous exclusion of air and water. Dry glovebox or Schlenk techniques were employed, using purified nitrogen or argon (H_2O and O_2 < 1 ppm). CH_3CN was rigorously dried by standard procedure, distilled, degassed prior to use, and stored under N_2 over molecular sieves. The water content in the CH_3CN was checked by coulometric Karl Fischer titration and has been found to be less than 5 ppm.

Sample Preparation. Acetonitrile solutions of $[Ln(CH_3CN)_9][Al(OC(CF_3)_3)_4]_3$ (Ln = Gd^{3+}, Eu^{3+}) were prepared by dissolving the solid lanthanide salts in pure, anhydrous acetonitrile.[24] The acetonitrile solution of $[Eu(CH_3CN)_9][Al(OC(CF_3)_3)_4]_2$ was obtained by passing the acetonitrile solution of $[Eu(CH_3CN)_9][Al(OC(CF_3)_3)_4]_3$ at least 7 times over a glass column filled with Zn/Hg amalgam.[25] The concentration of the paramagnetic metal in the solutions was determined using the bulk magnetic susceptibility shift of the ^1H NMR signal of TMS (see Supporting Information). The presence of the diamagnetic Zn^{2+} ions in the solution, produced by the reduction of europium(III) to europium(II), has no influence on ^{14}N or ^1H NMR relaxation.

^{14}N NMR. Longitudinal, $1/T_1$, and transverse, $1/T_2$, ^{14}N NMR relaxation rates as well as chemical shift measurements on $[Gd(CH_3CN)_9][Al(OC(CF_3)_3)_4]_3$ (c_{Gd}= 1.34 mmol kg^{-1}) and $[Eu(CH_3CN)_9][Al(OC(CF_3)_3)_4]_2$ (c_{Eu} = 17.43 mmol kg^{-1}) were performed at temperatures between 228.15 and 349.15 K on Bruker ARX-400 (9.4 T, 28.9 MHz) and Avance II-800 (18.8 T, 57.8 MHz) spectrometers. The temperature was controlled by Bruker BVT-3000 control units and measured by the substitution technique.[26] To avoid susceptibility corrections to the chemical shifts, all samples were sealed under vacuum in glass spheres fitting into 10 mm NMR tubes.[27,28] $1/T_1$ and $1/T_2$ were measured using the inversion-recovery[29] and the Carr–Purcell–Meiboom–Gill[30] techniques, respectively. Reduced relaxation rates and chemical shifts were obtained using neat acetonitrile as reference.

^{1}H NMRD. Longitudinal ^1H relaxation rates were measured on solutions of $[Gd(CH_3CN)_9][Al(OC(CF_3)_3)_4]_3$ (c_{Gd} = 8.58 mmol L^{-1}, T = 238.15, 268.65, 298.15 and 319.15 K) and of $[Eu(CH_3CN)_9][Al(OC(CF_3)_3)_4]_2$ (c_{Eu} = 12.95 mmol L^{-1}, T = 238.15, 268.65 and 298.15 K). The measurements were performed on a Stelar Spinmaster FFC (Fast Field Cycling) relaxometer covering a continuum of magnetic fields from 7×10^{-4} to 0.47 T (corresponding to a proton Larmor frequency range of 0.01–20 MHz). The temperature was regulated by an air or N_2 gas flow using a Stelar VTC90 temperature control unit. At fields above 0.47 T, the measurements were performed on Bruker spectrometers: Avance 200 (2.3 T, 100 MHz; 4.7 T, 200 MHz), ARX-400 (9.4 T, 400 MHz), and Avance II-800 (18.8 T, 800 MHz). In all cases the temperature was measured by the substitution technique.[26] The samples were placed in cylindrical sample tubes or glass spheres placed into 10 mm NMR tubes. The magnetic field independent ^1H relaxation rates of neat acetonitrile were measured at 4.7 T: 0.104 s^{-1} (238.15 K), 0.077 s^{-1} (268.65 K), 0.068 s^{-1} (298.15 K), and 0.065 s^{-1} (319.15 K).

EPR Spectroscopy. EPR spectra of solutions of $[Gd(CH_3CN)_9][Al(OC(CF_3)_3)_4]_3$ (c_{Gd} = 19.23 mmol kg^{-1}) and $[Eu(CH_3CN)_9][Al(OC(CF_3)_3)_4]_2$ (c_{Eu} = 17.43 mmol kg^{-1}) were recorded in continuous wave mode at Q- (35 GHz) and X-band (9.4 GHz) on a Bruker ELEXSYS E500 spectrometer at temperatures between 231 and 331 K. A controlled N_2 gas flow was used to regulate temperature, measured by the substitution technique.[26] The microwave frequency was measured using a frequency counter embedded in the standard microwave bridge (X-band) or an external Hewlett-Packard 5353B frequency counter (Q-band).

Data Analysis. The simultaneous least-squares fits of ^{14}N NMR, ^1H NMRD, and EPR data were performed by the Visualizeur/Optimiseur programs[31] running on a Matlab 6.5 platform. The errors of the fitted parameters correspond to one standard deviation. The EPR spectra were analyzed by fitting with derivatives of the Lorentzian function using the NMRICMA program[32] for Matlab.

DATA TREATMENT AND RESULTS

To determine the dynamics of solvated complexes of lanthanide ions in solution we followed the strategy used to study lanthanide aqua ions[14] and gadolinium complexes.[33] The main information is obtained from nuclear spin relaxation and chemical shift measured on the nucleus directly bound to the paramagnetic ion; in the case of water this is ^{17}O. In the case of acetonitrile this is one of the two NMR active nuclei, ^{14}N or ^{15}N. To avoid working with isotopically enriched samples we chose ^{14}N which has a >99% natural abundance. Because of very fast exchange of solvent molecules between the first coordination sphere and the bulk, only a coalesced NMR signal can be observed. The broadening and the chemical shift of this signal reflects, besides the amount of bound solvent, the exchange rate constant, the relaxation in the bound state, and the chemical shift difference between bound and bulk solvent.[34] The latter two properties are intrinsically linked to paramagnetic properties of the ion like the magnetic moment and electron spin relaxation. Extracting the desired dynamic parameters like the exchange rate constant, k_{ex}, and the rotational correlation time, τ_R, needs knowledge on many other parameters like the metal-nitrogen distance, the electron spin relaxation rates, $1/T_{1e}$ and $1/T_{2e}$, or the quadrupolar coupling constant of ^{14}N in CH_3CN. To reduce the strong correlation between the parameters in the data fitting process we developed a combined analysis of data from different NMR techniques together with EPR line width.[33]

The temperature variation of the relaxation enhancement and the chemical shift due to the presence of paramagnetic ions has been developed about 50 years ago.[1,2,35] The basic equations are repeated here for convenience, the full set of equations being given in the Supporting Information.

^{14}N NMR. The reduced relaxation rates ($1/T_{1r}$, $1/T_{2r}$) and chemical shift ($\Delta\omega_r$) of the coalesced ^{14}N NMR signal of $[M(CH_3CN)_9]^{n+}$ and bulk CH_3CN are given by eqs (1) to (4).

$$\frac{1}{T_{1r}} = \frac{1}{P_m}\left[\frac{1}{T_1} - \frac{1}{T_{1A}}\right] = \frac{1}{T_{1m} + \tau_m} \tag{1}$$

$$\frac{1}{T_{2r}} = \frac{1}{P_m}\left[\frac{1}{T_2} - \frac{1}{T_{2A}}\right] = \frac{1}{\tau_m}\frac{T_{2m}^{-2} + T_{2m}^{-1}\tau_m^{-1} + \Delta\omega_m^2}{(T_{2m}^{-1} + \tau_m^{-1})^2 + \Delta\omega_m^2} \tag{2}$$

$$\Delta\omega_r = \frac{1}{P_m}[\omega - \omega_A] = \frac{\tau_m^{-2}\Delta\omega_m}{(T_{2m}^{-1} + \tau_m^{-1})^2 + \Delta\omega_m^2} \tag{3}$$

$$P_m = \frac{q[M^{n+}]}{24.36\ \text{mol kg}^{-1}} \tag{4}$$

The relaxation and chemical shift of the bulk CH_3CN are marked with the index A and are obtained from a neat acetonitrile sample. Relaxation and shift of CH_3CN bound to the metal ion are marked with the index m. The residence time of a solvent molecule in the bound state, τ_m, is the inverse of the exchange rate constant for a particular coordinated solvent molecule:[20] $\tau_m = 1/k_{ex}$. The mole fraction of bound solvent, P_m, is the number of coordinated solvent molecules, q, times the concentration of the metal (in molality) divided by the number of moles CH_3CN per kg of solvent.

The relaxation of ^{14}N spins bound to the isoelectronic Gd^{3+} or Eu^{2+} is governed by dipolar, scalar, and quadrupolar relaxation (see Supporting Information). The first two of these relaxation mechanisms depend on the electron spin relaxation. Rast et al. developed a refined theoretical description of electron spin relaxation of the $S = 7/2$ ion including static and transient zero-field splitting.[36]

^{1}H Nuclear Magnetic Relaxation Dispersion. The magnetic field dependence of the longitudinal ^{1}H relaxation, measured over a wide range of magnetic field, is commonly designed as Nuclear Magnetic Relaxation Dispersion (NMRD).[37,38] The $1/T_1$ relaxation enhancement for a 1 mM solution of the paramagnetic ion is commonly named relaxivity, r_1 (eq 5).

$$r_1 = \frac{1}{[M^{n+}]}\left[\frac{1}{T_1} - \frac{1}{T_{1A}}\right];\quad [M^{n+}]\text{: concentration in mM} \tag{5}$$

Please note that for dilute aqueous solutions the molarity and the molality scales are equal in the mM range. For acetonitrile with a density of 0.786 kg dm^{-3} (at 20 °C) a 1 mM solution corresponds to 1.276 mmol kg^{-1}. For our diluted solutions we approximate the density by the density of neat CH_3CN. The relaxivity can be separated in an inner-sphere, r_1^{IS}, and an outer-sphere, r_1^{OS}, contribution (see Supporting Information). The inner-sphere relaxivity, which is due to solvent molecules directly bound to the metal ion, can be calculated using similar parameters as for ^{14}N NMR, besides there is no quadrupolar contribution and the distance to be considered is the metal-CH_3-proton distance.

EPR Spectroscopy. As already mentioned Gd^{3+} and Eu^{2+} are isoelectronic and have electron spins $S = 7/2$. The EPR spectra of both complexes are interpreted as superimposed isotropic hyperfine structures of the naturally abundant isotopes ^{151}Eu (natural abundance $n = 47.82\%$, $I = 5/2$, $\gamma = 6.55 \times 10^7$ T^{-1} s^{-1}) and ^{153}Eu ($n = 52.18\%$, $I = 5/2$, $\gamma = 2.94 \times 10^7$ T^{-1} s^{-1}) and of ^{155}Gd ($n = 14.8\%$, $I = 3/2$, $\gamma = -0.83 \times 10^7$ T^{-1} s^{-1}) and ^{157}Gd ($n = 15.65\%$, $I = 3/2$, $\gamma = -1.08 \times 10^7$ T^{-1} s^{-1}). For Gd^{3+} only a coalesced resonance with non-Lorentzian shape has been observed. For Eu^{2+}, which has a larger hyperfine coupling constant, the splitting is clearly visible at high temperatures in the Q-band (Figure 1). The fitted hyperfine coupling constants are given in Table 1. The values found are very similar to those obtained earlier on the europium aqua ion[16] and on the gadolinium complex [Gd(TPATCN)].[39] Mainly because of the very narrow line width, the hyperfine coupling constants for $[Eu(CH_3CN)_9]^{2+}$ are much more precise than those for $[Eu(H_2O)_7]^{2+}$.

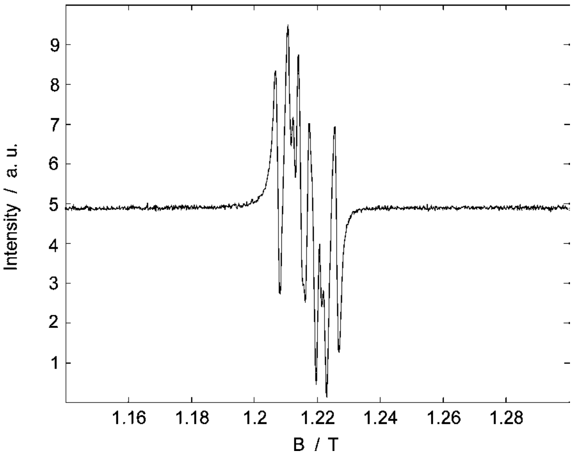

Figure 1. Q-band EPR spectrum of $[Eu(CH_3CN)_9][Al(OC(CF_3)_3)_4]_2$ in anhydrous acetonitrile at 318 K.

Table 1. Hyperfine Coupling Constants for Eu^{2+} and Gd^{3+} in Acetonitrile Complexes

isotope	$[M(CH_3CN)_9]^{n+\,a}$	$[Eu(H_2O)_7]^{2+\,b}$	$[Gd(TPATCN)]^{c}$
	Hyperfine Coupling Constant $A/g\mu_B$ (G)		
^{151}Eu	37.3 ± 0.01	37.3 ± 1	
^{153}Eu	16.6 ± 0.02	16.4 ± 1	
^{155}Gd	4.77 ± 0.11		4.34[d]
^{157}Gd	6.06 ± 0.07		5.67[e]

[a] At 331 K, this work. [b] At 365 K, ref 16. [c] Reference 39. [d] At 342.5 K. [e] Calculated from ^{155}Gd.

The electron spin relaxation in metal ions with $S \geq 1$ is dominated by zero-field splitting (ZFS) interactions. The basic theory for $S = 7/2$ has been developed by Hudson and Lewis.[40] Fries and co-workers[36,41] developed a refined description using a static and a transient ZFS. Peak-to-peak widths of the experimental derivative spectrum, ΔH_{pp}, have been obtained by using the Rast–Fries–Borel model[41,42] within the Redfield limit including the hyperfine splitting (see Supporting Information).

Results. Experimental results of ^{14}N NMR and EPR peak-to-peak linewidths for $[Gd(CH_3CN)_9]^{3+}$ and $[Eu(CH_3CN)_9]^{2+}$

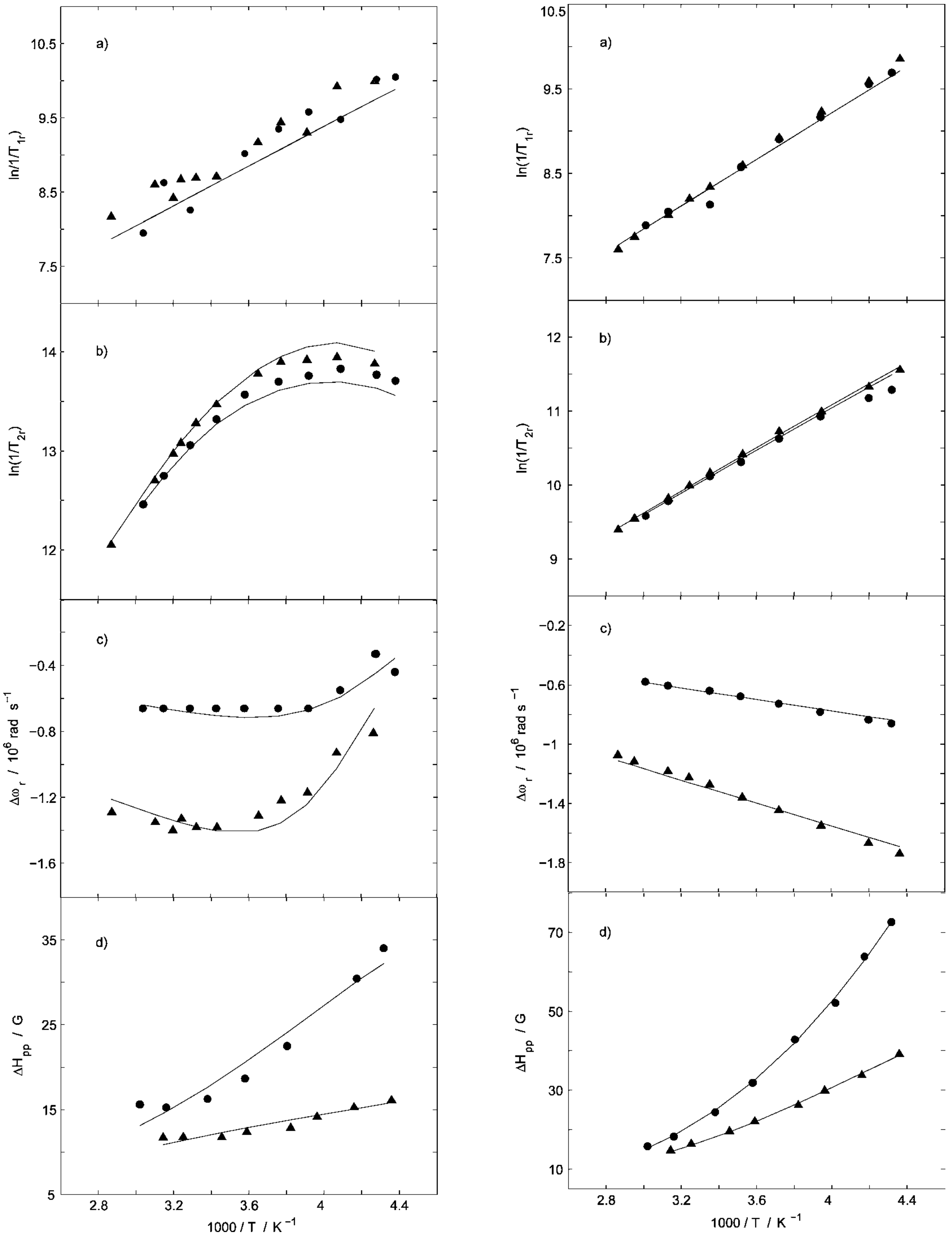

Figure 2. Temperature dependence of reduced longitudinal $\ln(1/T_{1r})$ (a) and transverse $(\ln(1/T_{2r})$ (b) ^{14}N relaxation rates and reduced chemical shifts $\Delta\omega_r$ (c) measured at B_0 = 9.4 T (●) and 18.8 T (▲) for $[Gd(CH_3CN)_9][Al(OC(CF_3)_3)_4]_3$ (left) and $[Eu(CH_3CN)_9][Al(OC(CF_3)_3)_4]_2$ (right); EPR peak to peak line widths ΔH_{pp} at X-band (●) and Q-band (▲) (d). The lines through the data points result from the combined least-squares fits using Rast−Borel equations.

are shown in Figure 2. Comparing the experimental data of the transverse relaxation, $\ln(1/T_{2r})$, and the chemical shift difference, $\Delta\omega_r$, for the $[Gd(CH_3CN)_9]^{3+}$ and the $[Eu(CH_3CN)_9]^{2+}$ compounds immediately reveals that the exchange on the triple charge ion is much slower than on the double charge one. Both results, $\ln(1/T_{2r})$ and $\Delta\omega_r$, show a changeover from fast to slow exchange for Gd^{3+} while Eu^{2+} shows fast exchange behavior over the whole temperature range studied.[34] From the bigger values of the longitudinal relaxation, $\ln(1/T_{1r})$, one can conclude qualitatively that the rotational correlation time is longer for $[Gd(CH_3CN)_9]^{3+}$ than for $[Eu(CH_3CN)_9]^{2+}$. NMRD profiles measured at four and three temperatures, respectively, are given in Figure 3. All profiles are typical for small, fast rotating complexes.

For both systems, simultaneous nonlinear least-squares fits of all experimental data (presented in Figures 2 and 3) have been performed, and the fitted parameters are shown in Table 2. Proton relaxivities only at resonance frequencies above 6 MHz were included in the fit to respect the validity of the high-field condition as given by Fries and Belorizky.[43,44] Simultaneous

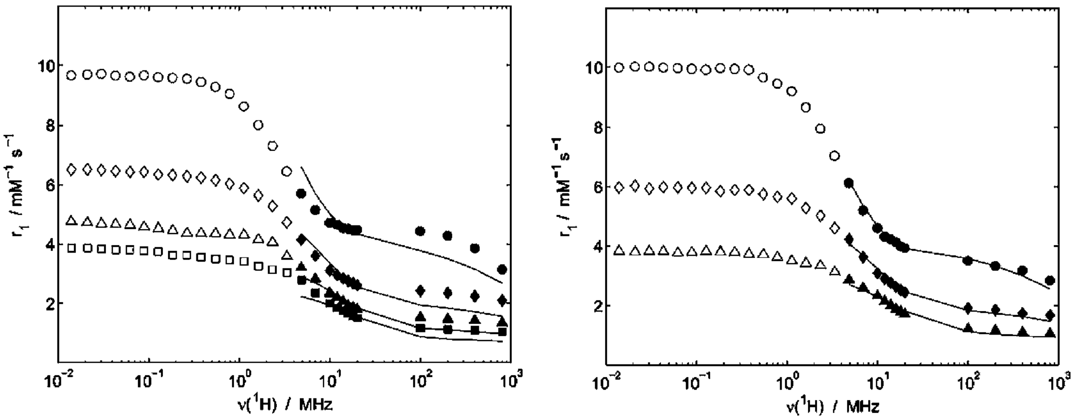

Figure 3. ^{1}H NMRD profiles of $[Gd(CH_3CN)_9][Al(OC(CF_3)_3)_4]_3$ (left) and $[Eu(CH_3CN)_9][Al(OC(CF_3)_3)_4]_2$ (right) at 238 K (○), 268.5 K (◇), 298 K (Δ), and 319 K (□). The lines through the data points result from the combined least-squares fits using Rast−Borel equations. Only high fields (full filled symbols) were considered for the simultaneous fit.

Table 2. Parameters Obtained from the Simultaneous Nonlinear Least Squares Fit of ^{14}N NMR, EPR, and ^{1}H NMRD Data.[a]

	$[Gd(CH_3CN)_9]^{3+}$	$[Eu(CH_3CN)_9]^{2+}$
$k_{ex}/10^6$ s^{-1}	54.9 ± 14.7	1530 ± 202
$\Delta H^‡$/kJ mol^{-1}	25.5 ± 4.5	9.1 ± 1.2
$\Delta S^‡$/J mol^{-1} K^{-1}	−11.1 ± 15.7	−36.2 ± 4.4
$(A/\hbar)/10^6$ rad s^{-1}	−3.2 ± 0.3	−2.5 ± 0.2
C_{os}	$\underline{0}$	$\underline{0.2}$
g	1.9927 ± 0.42	1.9933 ± 0.24
$\tau_R{}^{298}/10^{-12}$ s	14.5 ± 1.8	11.8 ± 1.1
E_R/kJ mol^{-1}	10.6 ± 1.4	11.3 ± 0.3
$\tau_v{}^{298}/10^{-12}$ s	0.11 ± 0.1	0.65 ± 0.1
E_v/kJ mol^{-1}	0.95 ± 1.8	14.2 ± 0.5
$a_2/10^{10}$ s^{-1}	0.048 ± 0.027	$\underline{0}$
$a_4/10^{10}$ s^{-1}	$\underline{0}$	$\underline{0}$
$a_6/10^{10}$ s^{-1}	0.005 ± 0.0007	0.007 ± 0.0008
$a_{2T}/10^{10}$ s^{-1}	0.65 ± 0.29	0.34 ± 0.02
$D_{LnH}{}^{298}/10^{-10}$ m^2 s^{-1} [b]	$\underline{43.7}$	$\underline{43.7}$
E_{DLnH}/kJ mol^{-1}	14.4 ± 4.8	13.7 ± 3.4
$(\chi^2(1+\eta^2/3))^{1/2}$/MHz	$\underline{4.5}$	$\underline{4.5}$
r_{LnN}/Å	2.4 ± 0.6	2.4 ± 0.4
$r_{LnH\ first\ sphere}$/Å	5.2 ± 1.1	5.3 ± 1.2
$a_{LnH\ bulk}$/Å	5.7 ± 5.0	±4.0

[a] Errors given correspond to one standard deviation; underlined values are fixed in the fitting procedure. [b] Fixed to the diffusion constant for neat CH_3CN.[46]

analysis of all data including the low frequency ^{1}H relaxivities gave no satisfactory fit for both ions, Gd^{3+} and Eu^{2+}. For extensive discussion of the validity of the simplified treatment of electron spin relaxation we refer to the recent publications of Fries and co-workers.[44,45] The curves calculated from the best fit parameters are shown in Figures 2 and 3.

The coordination number for acetonitrile on Gd^{3+} and Eu^{2+} enters directly in the evaluation of all experimental data except for the EPR line width, ΔH_{pp}. Because the coordination numbers of both ions could not be directly measured in solution some uncertainty concerning the fitted parameters presented in Table 2 exists. In the fitting procedure, in concordance with the solid state structure,[24] a coordination number $q = 9$ has been used. An extended X-ray absorption fine structure (EXAFS) study leads to a coordination number of 8 for Eu^{2+} and Sr^{2+}.[9] The authors used however an anion, $CF_3SO_3^-$, which was found to be coordinating in the weak solvent CH_3CN.[24] A parallel fit using $q = 8$ has been performed as well, leading to a 12% increase of the k_{ex}, τ_R, and $A/\hbar$ values which corresponds to the ratio of coordination numbers 9/8.

The distances between the paramagnetic center, which is assumed to be at the nucleus of the lanthanide ion, and the ^{14}N and ^{1}H nuclei have been adjusted in the fitting procedure. A Gd-N distance of 2.4 ± 0.6 Å was found which is shorter than the value from crystallographic data (2.55 Å).[24] It should however be kept in mind that the crystallographic distance was obtained from a partially optimized structure and was measured at 100 K. Baaden et al.[47] found from classical molecular dynamics simulation a distance of 2.45 to 2.50 Å for the trivalent europium which has an ionic radius similar to Gd^{3+}. Surprisingly, in the fitting procedure a similar distance was obtained for $[Eu(CH_3CN)_9]^{2+}$ as well: 2.4 ± 0.4 Å. If we take into account the larger ionic radius of 1.30 Å for Eu^{2+} compared to 1.107 Å for Gd^{3+} (both for $q = 9$) a larger distance should be observed for the double charged ion.[6] From an EXAFS study the Eu^{2+}-N distance has been determined to be 2.640 Å.[9] In a quantum chemical investigation it has been shown for $[Gd(H_2O)_8]^{3+}$ that the point-dipole model, which assumes that the electron spin is centered at the metal nucleus, is not strictly valid for the directly bound oxygen atoms.[48] Furthermore, the standard deviations calculated for the internuclear distances of ± 0.6 and ± 0.4 Å are relatively large and therefore the fitted distances have to be considered with caution.

The distance between the paramagnetic center and the ^{1}H nuclei of first coordination sphere CH_3CN molecules ($r_{LnH\ first\ sphere}$ in Table 2) is what can be expected from a radial alignment of the acetonitrile electric dipole. What is more surprising is the closest distance of approach to the paramagnetic ion for noncoordinated bulk CH_3CN molecules ($a_{LnH\ bulk}$): this distance which is calculated from the outer-sphere contribution to the ^{1}H relaxivity, is for both compounds close to $r_{LnH\ first\ sphere}$. A possible explanation is either a tangential or an antiparallel arrangement of second sphere or bulk solvent molecules in respect to first coordination sphere CH_3CN. Acetonitrile has a rod-like shape and therefore the nine coordinated complexes look like chestnut fruits: the surface has many voids allowing an easy and close approach of bulk solvent molecules. Results of a Monte Carlo simulation of alkali metal ions in acetonitrile show that solvent molecules in

Table 3. Rate Constants and Activation Parameters for Some Gd^{3+} and Eu^{2+} Solvation Complexes

	$k_{ex}^{298}/10^6$ s^{-1}	$\Delta H^‡$/kJ mol^{-1}	$\Delta S^‡$/J K^{-1} mol^{-1}	$\Delta V^‡/cm^3$ mol^{-1}	ref
$[Gd(CH_3CN)_9]^{3+}$	54.9	25.5	−11.1		this work
$[Gd(H_2O)_8]^{3+}$	804	15.3	−23.1	−3.3	33
$[Gd(DMSO)_8]^{3+}$	6.2	32.8	−4.7	+8.2	11
$[Eu(CH_3CN)_9]^{2+}$	1530	9.1	−36.2		this work
$[Eu(H_2O)_7]^{2+}$	5000	15.7	−7.0	−11.3	3,16

the second coordination sphere have an opposite dipolar orientation with the positively charged CH_3-group pointing toward the cation.[49] This result from computer simulation is supported by our experimental results on solutions of higher charged Gd^{3+} and Eu^{2+}-ions.

Different values for the ^{14}N quadrupolar coupling constant $(\chi^2(1+\eta^2/3))^{1/2}$ in CH_3CN can be found in literature ranging from 3.73 MHz (solid state)[50] to 4.22 MHz (gas phase).[51] After performing some preliminary fits with various quadrupolar coupling constants for ^{14}N, its value has finally been fixed to $(\chi^2(1+\eta^2/3))^{1/2} = 4.5$ MHz. For Gd^{3+} aqua complexes small changes of the quadrupolar coupling constant in respect to neat solvent values have been found.[52] It is clear that a strong correlation between the value of $(\chi^2(1+\eta^2/3))^{1/2}$ and those of τ_R, r_{LnN}, and $r_{LnH\ \text{first sphere}}$ exists.

The parameters for the static ZFS, a_2, a_4, a_6, and that of the transient ZFS, a_{2T}, were freely adjusted in a first fit. For both systems fitted a_4 values were close to zero and small compared to its standard deviation. We therefore set it to zero in the final fit. The same happened to the parameter a_2 in case of $[Eu(CH_3CN)_9]^{2+}$ and therefore it has been treated in the same way. The correlation times, τ_v, and its activation energies, E_v, obtained from the fits suffer from large statistical errors and should be regarded in our case as fitting parameters.

DISCUSSION

The ^{14}N longitudinal relaxation rates and the ^1H NMRD data at Larmor frequencies above 6 MHz are both hardly influenced by the electron spin relaxation. Both are dominated by the rotational correlation time τ_R which has been determined to the very short values of 14.5 and 11.8 ps for Gd^{3+} and Eu^{2+} complexes, respectively. Desreux and co-workers[53] determined $\tau_R = 51$ ps from a ^1H NMRD profile measured on a perchlorate solution. They admitted the presence of one ClO_4^- anion in the first coordination sphere and assumed a coordination number $q = 8$ for CH_3CN. They also assumed a much shorter residence time $\tau_m = 3000$ ps ($k_{ex} \sim 3.3\ 10^8\ s^{-1}$) for acetonitrile in the first coordination sphere than that measured in this work. The rotational correlation time determined for $[Gd(CH_3CN)_9]^{3+}$ (14.5 ps) is 2.8 times shorter than that measured for $[Gd(H_2O)_8]^{3+}$ (41 ps).[33] The shorter τ_R for acetonitrile very nicely reflects the lower viscosity: 0.35 cP for CH_3CN in respect to 0.89 cP for H_2O (both at 298 K). The correlation time of the divalent $[Eu(CH_3CN)_9]^{2+}$ is 20% shorter than that of the trivalent $[Gd(CH_3CN)_9]^{3+}$. This faster movement can be rationalized by a weaker interaction with second sphere solvent molecules for the lower charged solvate complex.

Comparing the experimental values of ΔH_{pp} measured at X-band and at Q-band for both ions with those of the corresponding aqua ions[16,36] one immediately sees that electron spin relaxation is much slower on the CH_3CN complexes. The CH_3CN and H_2O complexes of Gd^{3+} were both analyzed using the theory of Fries and co-workers with static and a transient ZFS. The static ZFS (a_2, a_4, a_6) is about an order of magnitude smaller for $[Gd(CH_3CN)_9]^{3+}$ than for $[Gd(H_2O)_8]^{3+}$; the amplitude for the transient ZFS (a_{2T}) is however similar. This finding strengthens the observation that binding of nitrogen leads to smaller ZFS than binding with oxygen atoms.[39] This observation has been rationalized by the smaller effect on the ligand field of the less electronegative nitrogen compared to an oxygen atom.

The exchange of acetonitrile on the homoleptic complexes of Gd^{3+} and Eu^{2+} is discussed first by comparing the tri- to the divalent complex and second by comparison to other solvents. The exchange on Eu^{2+} is about 30 times faster (at 300 K) than on Gd^{3+}. This can be safely attributed to the stronger electrostatic attraction of the smaller 3+ ion in respect to the bigger 2+ ion. The acceleration of the exchange reaction is only a factor of 6 for $[Eu(H_2O)_7]^{2+}$ in respect to $[Gd(H_2O)_8]^{3+}$. Comparing the exchange rate constant of CH_3CN to the corresponding rate constant of H_2O leads however to a surprising result: exchange of acetonitrile on Gd^{3+} is about 15 times slower than that of water. Following the solvent affinity sequence of Bünzli, DMSO > DMF ≈ $\mathbf{H_2O}$ > $(CH_3)_2CO$ > $\mathbf{CH_3CN}$,[4,8] water is a much better solvent for lanthanides than acetonitrile. The order of k_{ex} in respect to CH_3CN and DMSO (Table 3) is however well followed: DMSO, being the better solvent, exchanges ten times slower than acetonitrile. This suggests that an exceptional behavior is observed for the water exchange, which is much faster than it should be following its solvation properties. This exceptional behavior has already been stressed before by comparison with water exchange on poly(amino) carboxylate complexes and is due to the very low energy of the transition state in the associatively activated exchange reaction.[3]

Both activation entropies determined are negative (Table 3) and suggest therefore an associative activation mode for the solvent exchange reaction. The sign of $\Delta S^‡$ is, however, not a very reliable means to assign a reaction mechanism. First of all, the standard deviations from the data fitting are big (see Table 2) because $\Delta S^‡$ is obtained from extrapolation to infinite temperature. Second several examples can be found in literature[3] with different signs for $\Delta S^‡$ and for $\Delta V^‡$ both being in principle indicative for the reaction mechanism.[54] A prominent example is DMF exchange on lanthanides: for Tb^{3+} to Er^{3+} negative $\Delta S^‡$ are measured but a dissociative activation mode I_d has been assigned from the positive volumes of activation $\Delta V^‡$.[20] Variable pressure measurements would be a better tool to assign a reaction mechanism, but all attempts failed so far because of the extreme hygroscopy of the acetonitrile solutions. Another tool to assign a reaction mechanism is the determination of the rate law for the exchange reaction. This needs the use of an inert diluent not entering the first coordination sphere of the metal ion. However, acetonitrile is such a weak ligand that no such diluent exists and therefore the rate law could not be determined.

■ CONCLUSION

Variable magnetic field and temperature ^{14}N-, ^{1}H NMR and EPR experiments have been performed in anhydrous CH_3CN solutions of $[Gd(CH_3CN)_9]^{3+}$ and $[Eu(CH_3CN)_9]^{2+}$. For each system a combined analysis of all experimental data allowed to get microscopic information on the dynamics in solution. It has been found that the rotational diffusion as measured by the rotational correlation time is faster in the organic solvent than in water. The 2.8-fold acceleration corresponds to the lower viscosity of CH_3CN in respect to H_2O. Surprisingly, for both solvate complexes CH_3CN exchange is slower for the less strongly coordinated N-binding solvent than for more strongly coordinated O-binding H_2O. This could be explained by the exceptional behavior of water exchange on $[Gd(H_2O)_8]^{3+}$. For this compound the nine-coordinated transition state has a very low energy leading to a fast exchange following an associative activation mode. Solvent exchange on the divalent compound $[Eu(CH_3CN)_9]^{2+}$ is much faster than on the trivalent Gd-analogue. The difference of the exchange rate constants of CH_3CN and H_2O is much less pronounced on Eu^{2+} (acetonitrile is a factor of 3.3 slower than water) than on Gd^{3+} (acetonitrile is a factor of 15 slower than water).

Electron spin relaxation on both isoelectronic ions is much slower than on the oxygen binding water analogues. This allowed a precise determination of the hyperfine coupling constants for Gd^{3+} and Eu^{2+}. The found values are in good agreement with those determined earlier for other complexes.

■ ASSOCIATED CONTENT

Ⓢ Supporting Information

All equations used for the combined analysis and further details are given (Table SI-1)). This material is available free of charge via the Internet at http://pubs.acs.org.

■ AUTHOR INFORMATION

Corresponding Author

*Phone: +41 21 693 9876. Fax: +41 21 693 9855. E-mail: lothar.helm@epfl.ch.

Present Address

†ETHZ Laboratorium für Organische Chemie, HCI Hönggerberg, CH-8093 Zürich, Switzerland.

Notes

The authors declare no competing financial interest.

■ ACKNOWLEDGMENTS

Andre Merbach is acknowledged for numerous helpful and stimulating discussions as well as Alain Borel for his help with the EPR measurements. This work was supported by the Swiss National Science Foundation.

■ REFERENCES

(1) Swift, T. J.; Connick, R. E. *J. Chem. Phys.* **1962**, *37*, 307−320.

(2) Swift, T. J.; Connick, R. E. *J. Chem. Phys.* **1964**, *41*, 2553−2554.

(3) Helm, L.; Merbach, A. E. *Chem. Rev.* **2005**, *105*, 1923−1960.

(4) Bünzli, J.-C.; Milicic-Tang, A. Solvation and anion interaction in organic solvent. In *Hanbook on the Physics and Chemistry of Rare Earths*; Gschneider, K. A., Eyring, H., Eds.; Elsevier: Amsterdam, The Netherlands, 1995; Vol. *21*, pp 305−366

(5) Eliseeva, S. V.; Bünzli, J.-C. G. *Chem. Soc. Rev.* **2009**, *39*, 189−227.

(6) Shannon, R. D. *Acta Crystallogr., Sect. A* **1976**, *32*, 751−767.

(7) Seitz, M.; Oliver, A. G.; Raymond, K. N. *J. Am. Chem. Soc.* **2007**, *129*, 11153−11160.

(8) Bünzli, J.-C. G.; Vuckovic, M. M. *Inorg. Chim. Acta* **1983**, *73*, 53−61.

(9) Moreau, G.; Scopelliti, R.; Helm, L.; Purans, J.; Merbach, A. E. *J. Phys. Chem. A* **2002**, *106*, 9612−9622.

(10) Tobe, M. L.; Burgess, J. *Inorganic Reaction Mechanisms*; Addison Wesley: New York, 1999.

(11) Dessapt, R.; Helm, L.; Merbach, A. E. *J. Phys.:Condens. Matter* **2004**, *16*, S1027−S1032.

(12) Cossy, C.; Helm, L.; Merbach, A. E. *Inorg. Chem.* **1988**, *27*, 1973−1979.

(13) Cossy, C.; Helm, L.; Merbach, A. E. *Inorg. Chem.* **1989**, *28*, 2699−2703.

(14) Micskei, K.; Powell, D. H.; Helm, L.; Brücher, E.; Merbach, A. E. *Magn. Reson. Chem.* **1993**, *31*, 1011−1020.

(15) Caravan, P.; Merbach, A. E. *Chem. Commun.* **1997**, 2147−2148.

(16) Caravan, P.; Tóth, É.; Rockenbauer, A.; Merbach, A. E. *J. Am. Chem. Soc.* **1999**, *121*, 10403−10409.

(17) Pisaniello, D. L.; Helm, L.; Meier, P. F.; Merbach, A. E. *J. Am. Chem. Soc.* **1983**, *105*, 4528−4536.

(18) Pisaniello, D. L.; Helm, L.; Zbinden, D.; Merbach, A. E. *Helv. Chim. Acta* **1983**, *66*, 1872−1875.

(19) Powell, D. H.; Merbach, A. E. *Magn. Reson. Chem.* **1994**, *32*, 739−745.

(20) Lincoln, S. F.; Merbach, A. E. *Adv. Inorg. Chem.* **1995**, *42*, 1−88.

(21) Tóth, É.; Burai, L.; Merbach, A. E. *Coord. Chem. Rev.* **2001**, *216*−*217*, 363−382.

(22) Moreau, G.; Helm, L.; Purans, J.; Merbach, A. E. *J. Phys. Chem. A* **2002**, *106*, 3034−3043.

(23) Di Bernardo, P.; Choppin, G. R.; Portanova, R.; Zanonato, P. L. *Inorg. Chim. Acta* **1993**, *207*, 85−91.

(24) Bodizs, G.; Raabe, I.; Scopelliti, R.; Krossing, I.; Helm, L. *Dalton Trans.* **2009**, 5137−5147.

(25) Clerc, S. D.; Jewsbury, R. A.; Mortimer, M. G.; Zeng, J. *Anal. Chim. Acta* **1997**, *339*, 225−229.

(26) Ammann, C.; Meier, P.; Merbach, A. E. *J. Magn. Reson.* **1982**, *46*, 319−321.

(27) Hugi, A. D.; Helm, L.; Merbach, A. E. *Helv. Chim. Acta* **1985**, *68*, 508−521.

(28) Micskei, K.; Helm, L.; Brücher, E.; Merbach, A. E. *Inorg. Chem.* **1993**, *32*, 3844−3850.

(29) Vold, R. L.; Waugh, J. S.; Klein, M. P.; Phelps, D. E. *J. Chem .Phys.* **1968**, *48*, 3831−3832.

(30) Meiboom, S.; Gill, D. *Rev. Sci. Instrum.* **1958**, *29*, 688−691.

(31) Yerly, F. *Visualiseur/Optimiseur*, 2.3.6; EPFL: Lausanne, Switzerland, 2003.

(32) Helm, L.; Borel, A.; Yerly, F. *NMRICMA*, 3.0.4; EPFL: Lausanne, Switzerland, 2004.

(33) Powell, D. H.; Ni Dhubhghaill, O. M.; Pubanz, D.; Helm, L.; Lebedev, Y. S.; Schlaepfer, W.; Merbach, A. E. *J. Am. Chem. Soc.* **1996**, *118*, 9333−9346.

(34) Helm, L.; Nicolle, G. M.; Merbach, A. E. *Adv. Inorg. Chem.* **2005**, *57*, 327−379.

(35) Luz, Z.; Meiboom, S. *J. Chem. Phys.* **1964**, *40*, 2686−2693.

(36) Rast, S.; Borel, A.; Helm, L.; Belorizky, E.; Fries, P. H.; Merbach, A. E. *J. Am. Chem. Soc.* **2001**, *123*, 2637−2644.

(37) Koenig, S. H.; Brown, R. D., III, Relaxivity of MRI magnetic contrast agents. Concepts and principles. In *Handbook of metal-ligand interactions in biological fluids. Bioinorganic chemistry*; Berthon, G., Ed.; Dekker: New York, 1995; pp 1093−1108.

(38) Bertini, I.; Luchinat, C.; Parigi, G. *Solution NMR of Paramagnetic Molecules*; Elsevier: Amsterdam, The Netherlands, 2001; Vol. 2.

(39) Borel, A.; Kang, H.; Gateau, C.; Mazzanti, M.; Clarkson, R. B.; Belford, R. L. *J. Phys. Chem. A* **2006**, *110*, 12434−12438.

(40) Hudson, A.; Lewis, J. W. *Trans. Faraday Soc.* **1970**, *66*, 1297−1301.

(41) Rast, S.; Belorizky, E.; Fries, P. H.; Travers, J. P. *J. Phys. Chem. B* **2001**, *105*, 1978−1983.

(42) Borel, A.; Tóth, É.; Helm, L.; Merbach, A. E. *Phys. Chem. Chem. Phys.* **2000**, *2*, 1311−1317.

(43) Fries, P. H.; Belorizky, E. *J. Chem. Phys.* **2007**, *126*, 204503/1−13.

(44) Bonnet, C. l. S.; Fries, P. H.; Gadelle, A. e.; Gambarelli, S.; Delangle, P. *J. Am. Chem. Soc.* **2008**, *130*, 10401−10413.

(45) Belorizky, E.; Fries, P. H.; Helm, L.; Kowalewski, J.; Kruk, D.; Sharp, R. R.; Westlund, P.-O. *J. Chem. Phys.* **2008**, *128*, 052307.

(46) Holz, M.; Weingärtner, H. *J. Magn. Reson.* **1991**, *92*, 115−125.

(47) Baaden, M.; Berny, F.; Madic, C.; Wipff, G. *J. Phys. Chem. A* **2000**, *104*, 7659−7671.

(48) Yazyev, O. V.; Helm, L.; Malkin, V. G.; Malkina, O. L. *J. Phys. Chem. A* **2005**, *109*, 10997−11005.

(49) Fischer, R.; Richardi, J.; Fries, P. H.; Krienke, H. *J. Chem. Phys.* **2002**, *117*, 8467−8479.

(50) Casabella, P. A.; Bray, P. J. *J. Chem. Phys.* **1958**, *29*, 1105−1107.

(51) Kemp, M. K.; Pochan, J. M.; Flygare, W. H. *J. Phys. Chem.* **1967**, *71*, 765−767.

(52) Yazyev, O. V.; Helm, L. *J. Chem. Phys.* **2006**, *125*, 054503.

(53) Lambert, B.; Jacques, V.; Shivanyuk, A.; Matthews, S. E.; Tunayar, A.; Baaden, M.; Wipff, G.; Böhmer, V.; Desreux, J. F. *Inorg. Chem.* **2000**, *39*, 2033−2041.

(54) Langford, C. H.; Gray, H. B. *Ligand Substitution Processes*; W.A. Benjamin, Inc.: New York, 1965.